nature communications

Article

https://doi.org/10.1038/s41467-025-62380-y

Anti-CV2/CRMP5 autoantibodies as drivers of sensory neuron excitability and pain in rats

Received: 7 May 2024

Accepted: 18 July 2025

Published online: 07 August 2025

Check for updates

Laurent Martin[1,2,6], Harrison J. Stratton[1,6], Lyuba Y. Salih[3], Nicolas LA. Dumaire[3], Kimberly Gomez[1], Le Duy Do[4], Santiago Loya-Lopez[1], Cheng Tang[1], Aida Calderon-Rivera[1], Dongzhi Ran[1], Venkatrao Nunna[3], Shreya S. Bellampalli[1], Liberty François-Moutal[1,3], Shizhen Luo[1], Frank Porreca[1], Mohab Ibrahim[1,2], Véronique Rogemond[4], Jérôme Honnorat[4], Rajesh Khanna[1,5,7] & Aubin Moutal[1,3,7]

Paraneoplastic neurological syndromes arise from autoimmune reactions against nervous system antigens due to a maladaptive immune response to a peripheral cancer. Patients with small cell lung carcinoma or malignant thymoma can develop an autoimmune response against the CV2/collapsin response mediator protein 5 (CRMP5) antigen, with approximately 80% of these patients experiencing painful neuropathies. Here we investigate the mechanisms underlying anti-CV2/CRMP5 autoantibodies (CV2/CRMP5-Abs)-related pain and find that patient-derived CV2/CRMP5-Abs bind to their target on rat dorsal root ganglia (DRG) and superficial laminae of the spinal cord, to induce DRG neuron hyperexcitability and mechanical hypersensitivity. These effects from patient-derived Abs are recapitulated in rats immunized with a DNA vaccine for CRMP5, in which therapeutic treatment with anti-CD20 depleting B cells ameliorates autoimmunity and neuropathy. Our data thus reveal a mechanism of neuropathic pain in patients with paraneoplastic neurological syndromes and implicates CV2/CRMP5-Abs as a potential target for treating paraneoplastic neurological syndromes.

Paraneoplastic neurological syndromes manifest as autoimmune reactions against nervous system antigens triggered by a maladaptive immune response to a peripheral cancer[1]. Patients with small cell lung carcinoma or malignant thymoma can develop an autoimmune paraneoplastic syndrome with anti-CV2/collapsin response mediator protein 5 (CRMP5) autoantibodies (CV2/CRMP5-Abs)[2–4]. Among other symptoms, such as encephalitis, myelopathy, or cerebellar ataxia, 80% of patients with CV2/CRMP5-Abs also experience idiopathic painful neuropathy, often manifesting as symmetric or asymmetric polyradiculoneuropathy[2]. Pain frequently serves as the initial symptom that prompts patients to seek medical attention, ultimately leading to the diagnosis of their autoimmune disease[5]. The remarkably high prevalence of pain in this patient population surpasses that of many other well-

[1]Department of Pharmacology, College of Medicine, The University of Arizona, Tucson, AZ, USA. [2]Department of Anesthesiology, College of Medicine, The University of Arizona, Tucson, AZ, USA. [3]Department of Pharmacology and Physiology, School of Medicine, Saint Louis University, St. Louis, MO, USA. [4]French Reference Center for Paraneoplastic Neurological Syndromes and Autoimmune Encephalitis, Hospices Civils de Lyon, MeLiS—UCBL-CNRS UMR 5284—INSERM U1314, Université Claude Bernard Lyon 1, Lyon, France. [5]Department of Pharmacology & Therapeutics and Pain and Center for Advanced Pain Therapeutics and Research (CAPTOR), College of Medicine, University of Florida, Gainesville, FL, USA. [6]These authors contributed equally: Laurent Martin, Harrison J. Stratton. [7]These authors jointly supervised this work: Rajesh Khanna, Aubin Moutal. e-mail: aubin.moutal@health.slu.edu

characterized pain-related diseases, which present with associated pain[6–8].

Our goal was to understand how anti-CV2/CRMP5 autoimmunity causes neuropathic pain. Additionally, we aimed to develop a new model of anti-CV2/CRMP5 painful neuropathy, reproducing the pain symptoms observed in patients, allowing mechanistic investigation and assessment of possible therapeutic interventions. Human CV2/CRMP5-Abs have been shown to bind to human dorsal root ganglia (DRG) where sensory neurons are located[4,5]. CRMP5 is the most distant member (<50% homology) of the collapsin response mediator protein family[9,10] and is highly expressed in the central nervous system during embryonic development[11] where it regulates dendritic growth and Purkinje cell maturation[12,13]. After birth, CRMP5 expression is down-regulated but retained in the midbrain[11], DRG, and spinal cord[10]. While patients with anti-CV2/CRMP5 paraneoplastic neurological syndrome commonly present primarily with pain, the possible contribution of CRMP5 expression or function to pain has not been explored. Importantly, immunotherapy aimed at reducing autoantibody levels has been reported to reduce pain[2] in these patients, which suggests a possible interaction between circulating Abs and pain-sensing neurons.

From this evidence, we postulate that CV2/CRMP5-Abs might directly sensitize sensory neurons, which ultimately leads to enhanced pain. CV2/CRMP5-Abs were originally described as targeting an unknown 66 kDa cytoplasmic protein in the cerebellum and spinal cord[14], later identified as CRMP5[11,15–17]. CRMP5 is the most distant member (<50% homology) of the collapsin response mediator protein family[9,10] and is highly expressed in the nervous system during embryonic development[11] where it regulates dendritic growth and Purkinje cell maturation[12,13]. After birth, CRMP5 expression is down-regulated but retained in the midbrain[11], DRG, and spinal cord[10]. While CV2/CRMP5-Abs are largely associated with pain, CRMP5 expression or function is not known in the pain pathway. However, the CRMP5 gene (dpysl5) is cited among the key molecular contributors to the intensity of pain in veterans[18].

Here, our studies show that patient-derived CV2/CRMP5-Abs induce a hyperexcitability phenotype in cultured rodent DRG sensory neurons. Remarkably, this hyperexcitability correlates with heightened sensitivity to mechanical stimuli in rats. By immunizing rats against CRMP5, we can successfully replicate the pain phenotype observed in patients with CV2/CRMP5-Abs. Leveraging this reverse-translationally-informed model, we assess the effectiveness of common clinically used painkillers and a monoclonal antibody (anti-CD20), potentially offering valuable treatment options for patients experiencing autoantibody-induced pain. More broadly, our work shows that peripheral cancers can sensitize primary afferent neurons, which could be relevant to other conditions where pain and cancer are coincident. Our DNA immunization model could serve as a platform for screening novel therapeutic agents to treat pain associated with other neoplastic syndromes.

Results

Serum from patients with CV2/CRMP5-Abs stains their target CRMP5 in dorsal root ganglia and spinal cord

The concomitant occurrence of CV2/CRMP5-Abs and pain symptoms suggests that these autoantibodies likely play a causal role in the pain experienced by patients[5]. To directly explore the relationship between CV2/CRMP5-Abs and pain, we initially investigated whether sera from patients could identify their target along the pain neuraxis. Previous studies have reported positive autoimmunoreactivity of anti-CV2/CRMP5 autoantibodies in various brain regions, including the brainstem and the cerebellum[14,15]. Additionally, there is evidence that these autoantibodies can stain the human sciatic nerve and the DRG[4,5]. We assembled a collection of sera from 22 patients diagnosed with both anti-CV2 autoantibodies and neuropathy (Table 1). Our cohort included samples from 16 males and 6 females, collected during diagnosis and preserved for research purposes. No apparent sex-based prevalence associated with the development of CV2/CRMP5-Abs was reported[2,15].

Table 1 | Anti-CV2/CRMP5 positive sera used in this study

Patient #	Sex	Type of neuropathy	Pain	Primary tumor	Age at diagnosis
1	M	Motor and sensory neuropathy	Yes	Small cell lung cancer	56
2	M	Sub-acute sensory neuropathy	Yes	Small cell lung cancer	75
3	M	Motor and sensory neuropathy	Yes	Small cell lung cancer	60
4	F	Peripheral neuropathy	Yes	Small cell lung cancer	70
5	F	Peripheral neuropathy	Yes	Small cell lung cancer	70
6	F	Sensory neuropathy and Lambert-Eaton syndrome	Yes	Small cell lung cancer	64
7	F	Sensory neuropathy and Lambert-Eaton syndrome	Yes	Small cell lung cancer	64
8	M	Peripheral neuropathy	Yes	NA	70
9	M	Sensory neuropathy (and cerebellar syndrome)	Yes	Small cell lung cancer	64
10	M	Motor and sensory neuropathy	Yes	Bladder	54
11	F	Motor and sensory neuropathy	Yes	unknown	55
12	M	Lambert-Eaton syndrome	Yes	Small cell lung cancer	78
13	F	Polyneuropathy	Yes	unknown	56
14	M	Sensory neuropathy	Yes	Non-small cell lung cancer	76
15	M	Sensory neuropathy	Yes	unknown	62
16	M	cerebellar syndrome	No	Small cell lung cancer	63
17	M	Sensory neuropathy	No	Small cell lung cancer	56
18	M	Sensory neuropathy	No	Small cell lung cancer	80
19	M	Motor and sensory neuropathy	No	Small cell lung cancer	62
20	M	encephalitis	No	intestinal	69
21	M	Sensory neuropathy	No	Small cell lung cancer	45
22	M	Motor and sensory neuropathy	No	Small cell lung cancer	60

Sex, origin of the primary tumor, and age at diagnosis are indicated. All patients had a type of neuropathy, and those who reported pain are indicated.

https://doi.org/10.1038/s41467-025-62380-y

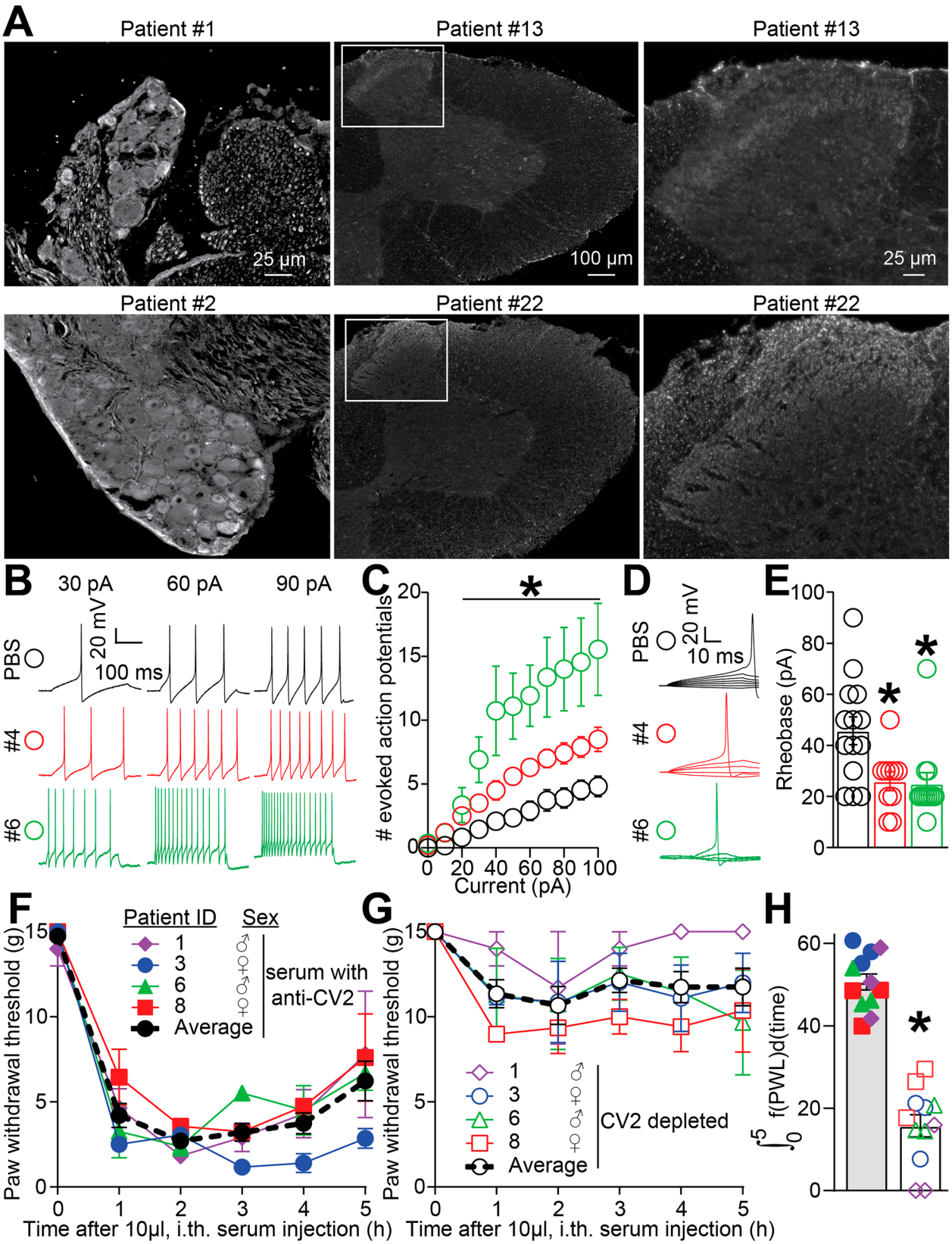

We found that sera from patients exhibited positive staining in the neuronal somata of rat DRG neurons (Fig. 1A). Additionally, strong labeling was observed in the spinal dorsal horn, where nociceptive neurons synapse onto second-order neurons (Figs. 1A and S1). This signal was specifically localized to laminae I and IIo of the dorsal spinal cord, suggesting that CV2/CRMP5-Abs may identify nociceptive fibers[19]. To further investigate this immunoreactivity, we conducted additional co-staining using a validated anti-CRMP5 antibody[20] (Fig. S1). While a control serum from a CV2/CRMP5-Abs-negative patient showed no staining, we observed comparable staining patterns between CV2/CRMP5-Abs and CRMP5 in the rat DRG and spinal dorsal horn, strongly suggesting that the observed immunoreactivity is

Fig. 1 | CV2/CRMP5-Abs labels nociceptive structures and induces mechanical hypersensitivity and DRG neuron hyperexcitability. A Micrographs of rat dorsal root ganglia (DRG) and spinal cord immunolabelled with anti-CV2 sera from three patients. The right panels show a magnification of boxed regions of spinal cord sections. The experiment was repeated across five rats with consistent results. **B** Representative recordings of evoked action potentials recorded from small-diameter DRG neurons in response to depolarizing current injection of 30, 60, and 90 picoamperes (pA). Female rat DRG neurons were treated overnight with serum from patient #4 or #6 (1/100 dilution). **C** Quantification of the number of evoked action potentials in response to 0–100 pA of injected current. $^*p < 0.05$, multiple Mann–Whitney tests. PBS $n = 11$ cells, Patient #4 $n = 11$ cells, Patient #6 $n = 11$ cells, obtained from at least three rats. **D** Representative traces of rheobase recordings from cells treated with PBS, serum from patient #4, or #6. **E** Bar graph with scatter plot showing a decreased rheobase in neurons treated with serum from patient #4 or #6. PBS $n = 14$ cells, Patient #4 $n = 10$ cells, Patient #6 $n = 12$ cells; error bars indicate mean ± SEM, $^*p < 0.05$, Kruskal–Wallis test. **F** Graph showing the paw withdrawal threshold of male rats injected intrathecally (i.th.) with 10 μL of the indicated positive CV2/CRMP5-Abs or (**G**) depleted (cross-adsorbed with purified CRMP5) sera. $n = 12$; 3 rats per CV2/CRMP5-Abs serum; 4 different CV2/CRMP5-Abs sera. The black line shows the average of all patients tested. two-way ANOVA. **H** Bar graph with scatter plot showing the area under the curve for the data in (**F**, **G**), $^*p < 0.05$, two-tailed, Mann–Whitney test. All data are shown with error bars that indicate mean ± SEM. See Supplementary Data 1 for additional statistical details. Source data are provided as a Source Data file.

related to CRMP5. We also established that CRMP5 is present in human DRG neurons (Fig. S2).

The above results raise questions about how these autoantibodies may interact with neurons. To address this, we employed proximity ligation assay (PLA), a technique that permits detection of protein-protein interactions in situ at endogenous protein levels[21]. In rat sensory neurons exposed overnight to CV2/CRMP5-Abs, we observed positive human IgG/CRMP5 PLA signals only when we permeabilized fixed cells prior to immunostaining. This indicates that human autoantibodies can bind to intracellular autoantigens, at least within sensory neurons (Fig. S3). Sera from the same patients, depleted by pre-adsorption on magnetic beads coated with purified CRMP5, did not exhibit any staining (Fig. S3A). Additionally, we fractionated DRG neurons treated with patient serum to isolate cytosolic, membrane, nuclear, and cytoskeletal fractions. Notably, human autoantibodies were detected in the cytosol of neurons through immunoblotting (Fig. S3B) and confocal imaging (Fig. S3C, D). Altogether, these findings highlight that anti-CV2 autoantibodies can specifically identify their target autoantigen within the cytoplasm of DRG sensory neurons and spinal cord dorsal horn neurons.

We next explored whether CV2/CRMP5-Abs could alter the overall function of DRG neurons. Employing a functional fingerprinting technique called constellation pharmacology, we used live cell calcium imaging to detect changes directly related to the sensitization of pain-relevant receptors and ion channels[22,23]. This approach uses several agonists to ligand gated ion channels (AITC: TRPA1, noxious cold; ATP: P2X and P2Y, inflammation; menthol: TRPM8, innocuous cold; capsaicin: TRPV1, noxious heat) and G-protein coupled receptors (acetylcholine: mAChR; histamine: histamine receptors, itch) to identify functional sensory neuron populations involved in heat, cold, itch or inflammatory pain[23]. As a reference control, we compared the serum of a CV2/CRMP5-Abs-negative patient with sera from patients #3 and #6 (Fig. S4A). Surprisingly, CV2/CRMP5-Abs exposure overnight had no effect on the proportion of DRG neurons responding to more than one receptor agonist (Fig. S4B) or to each receptor agonist (Fig. S4C). Additionally, the peak calcium response to each compound remained unchanged (Fig. S4D). We further analyzed the peak response to a depolarizing stimulus within each functional sensory neuron subpopulation and found no alteration due to CV2/CRMP5-Abs exposure (Fig. S4E). Finally, assessing the size of DRG neurons in relation to their functional response revealed no significant difference (Fig. S4F).

CV2/CRMP5-Abs increase sensory neuron excitability and sensitize mechanical responses in rats

Because CV2/CRMP5-Abs label sensory neurons in the DRG and are associated with painful neuropathy in humans, we next investigated whether these autoantibodies could cause hyperexcitability of DRG neurons, a crucial feature of pain sensitization in both rodents and humans[24–26]. To explore this, we cultured rat DRG neurons and exposed them overnight to serum containing CV2/CRMP5-Abs. Using patch clamp electrophysiology, we recorded excitability by evoking action potentials through stepwise current injections. DRG neurons treated with CV2/CRMP5-Abs exhibited a significantly higher number of evoked action potentials compared to control neurons, starting at 30 pA (Fig. 1B, C). Moreover, the rheobase, which represents the current needed to elicit a single action potential, was lower in CV2/CRMP5-Abs-treated neurons (Fig. 1D, E). In summary, our data strongly suggest that CV2/CRMP5-Abs enhance the excitability of sensory neurons, potentially contributing to pain hypersensitivity.

We next asked if anti-CV2/CRMP5 autoantibodies could induce pain-like behaviors in rodents. Specifically, we focused on mechanical hypersensitivity, a common symptom observed in patients with neuropathic pain[27,28]. To assess this, we employed an intrathecal catheter to inject rats with patients' serum containing CV2/CRMP5-Abs, directly exposing the spinal cord and DRG, comparing it to antibody-depleted controls. We then used Von Frey filaments to measure the mechanical sensitivity of the hindpaw. Remarkably, all four sera tested lowered mechanical thresholds for at least 5 h, while antibody depletion effectively negated this effect (Fig. 1F–H). These findings demonstrate that CV2/CRMP5-Abs can sensitize the pain pathway, leading to the manifestation of mechanical hypersensitivity.

CV2/CRMP5-Abs bind to surface accessible epitopes on CRMP5

While our findings (Fig. 1) are compelling, they do not establish a causal link between CV2/CRMP5-Abs and neuronal sensitization or pain responses via their antigen-binding fragment (Fab). We used a peptide array approach to map the protein sequence of CRMP5 using 15-mer peptides with 3 amino acid increments. We consistently identified three distinct epitopes (Peptides 53, 94, and 146) (Fig. 2A), along with Peptide 142, that were recognized by sera from six of seven patients (sequences shown in Fig. S5). Notably, patient characteristics (age, sex, neuropathy type, and primary tumor) did not significantly impact epitope recognition (Table 1 and Fig. 2A). These four epitopes, uniquely associated with CRMP5 (PDB ID: 4B90[29],), are exposed on the protein's surface and accessible for binding by CV2/CRMP5-Abs under native conditions (Fig. S5B). We next employed epitope peptides to mask the Fab domain of CV2/CRMP5-Abs. Peptides 53, 142, and 146 were chosen for these experiments, while peptide 94 was excluded due to solubility issues. Employing an ELISA approach, we successfully blocked the Fab region of human autoantibodies using these epitope peptides (100 ng/ml each). This prevented their binding to the target protein CRMP5 (Fig. 2B). Intriguingly, purified CRMP5 at the same concentration exhibited a similar level of inhibition, with less than 25% residual binding (Fig. 2B). Furthermore, we confirmed that the epitope peptides 53, 142, and 146 effectively blocked CV2/CRMP5-Abs immunoreactivity to DRG neurons (Fig. 2C). In culture, while permeabilization was necessary to obtain CV2/CRMP5-Abs immunoreactivity,

https://doi.org/10.1038/s41467-025-62380-y

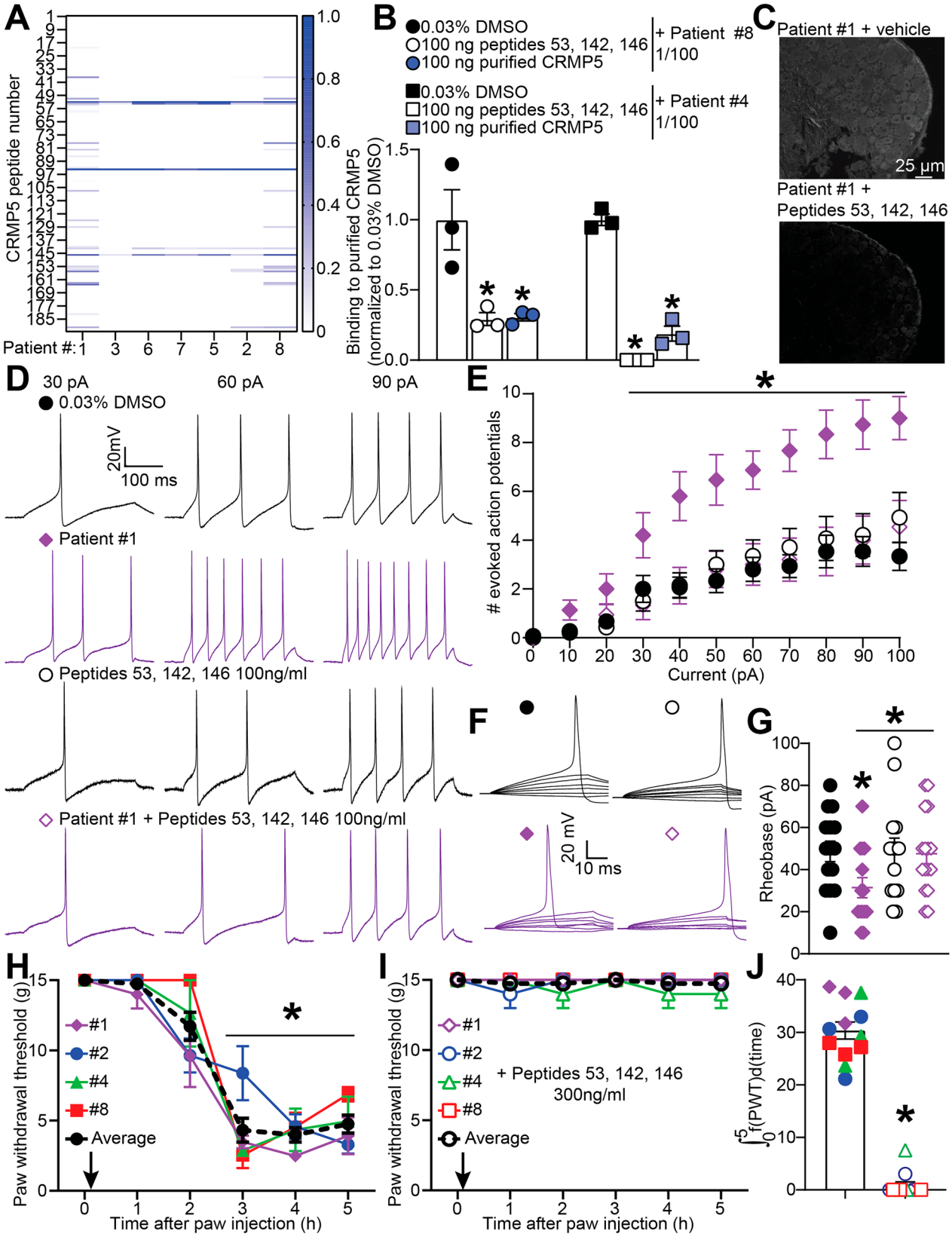

autoantibody binding was again blocked by the epitope peptides 53, 142, and 146 (Fig. S6). These findings demonstrate that CV2/CRMP5-Abs specifically bind to the peptide sequences 53, 142, and 146 on their target, CRMP5. Consequently, these peptides can be employed to prevent the binding of autoantibodies to their endogenous target.

Blocking CV2/CRMP5-Abs prevents DRG neuron excitability and mechanical hypersensitivity

To determine if the heightened excitability of DRG neurons exposed to CV2/CRMP5-Abs (Fig. 1D) was exclusively caused by these antibodies, we used peptides 53, 142, and 146 to block the Fab region. We treated cultured rat DRG neurons with whole serum (diluted 1/100) from

Fig. 2 | Blocking CV2/CRMP5-Abs with epitope peptides prevents the sensitization of sensory neurons and mechanical hypersensitivity in rats. A Heatmap of the immunoreactivity of CV2/CRMP5-Abs sera hybridized on a CRMP5 peptide array mapping the entire sequence of the protein in 15-mer peptides with three amino acid increments. Four main epitopes on CRMP5 are targeted by the CV2/CRMP5-Abs. **B** Bar graph with scatter plot showing that peptides 53, 142, and 146 can block the binding of CV2/CRMP5-Abs from patients #8 and #4 to purified CRMP5. 0.03% DMSO is the vehicle, purified CRMP5 was used as a positive control to achieve maximal displacement of the CV2/CRMP5-Abs. $n = 3$ independent measures from an average of three repeats. $^*p < 0.05$, one-way ANOVA. **C** Micrograph of a rat DRG immunolabelled with CV2/CRMP5-Abs positive serum (1/100) from patient #1 and then with blocking peptides 53, 142, 146. Blocking peptides abolished the immunoreactivity of CV2/CRMP5-Abs for their protein target CRMP5. The experiment was repeated across five rats with consistent results. **D** Representative recordings of evoked action potentials recorded from small-diameter DRG neurons treated with serum from patient #1 (1/100 dilution) in combination with 100 ng/ml of peptides 53, 142, and 146 as indicated, overnight in response to depolarizing current injection of 30, 60, and 90 pA. **E** Quantification of the number of evoked action potentials in response to 0–100 pA of injected current. $^*p < 0.05$, multiple Mann–Whitney tests. DMSO $n = 15$ cells, Patient #1 $n = 15$ cells, DMSO + peptides $n = 14$ cells, Patient #1 + peptides $n = 16$ cells. **F** Representative traces of rheobase recordings from cells treated with the serum from patient #1 and blocking peptides as indicated. **G** Bar graph with scatter plot showing unchanged rheobase in cells treated with the serum from patient #1 and with blocking peptides as indicated. $^*p < 0.05$, Kruskal–Wallis test. DMSO $n = 15$ cells, Patient #1 $n = 14$ cells, Patient #1 + peptides $n = 16$ cells from at least three rats. **H** Graph showing the paw withdrawal threshold of rats injected with 15 μl of the indicated CV2/CRMP5-Abs positive sera (1/10 dilution). **I** Graph showing the paw withdrawal threshold of rats injected with CV2/CRMP5-Abs positive sera with blocking peptides 53, 142, and 146 (300 ng/ml). $^*p < 0.05$, two-way ANOVA. **J** Bar graph with scatter plot showing the area under the curve of the data in (**H**, **I**) and color coded per treatment groups ($n = 3$ rats each), $^*p < 0.05$, Mann–Whitney. All data are shown with error bars that indicate mean ± SEM. Experimenters were blind to the treatment groups. See Supplementary Data 1 for additional statistical details. Source data are provided as a Source Data file.

patient #1 and added 100 ng/ml of the aforementioned peptides (Fig. 2D). Consistent with our previous observations (Fig. 1C), CV2/CRMP5-Abs increased sensory neuron firing frequency (Fig. 2D). Peptides 53, 142, and 146 (at 100 ng/ml) alone had no impact on action potential firing. However, sensory neuron hyperexcitability (Fig. 2D, E) and decreased rheobase (Fig. 2F, G) were successfully prevented by blocking the binding of autoantibodies using these peptides.

Next, we tested this approach in vivo with the aim of answering whether mechanical hypersensitivity induced by treatment with CV2/CRMP5-Abs was mediated exclusively by the Fab region of autoantibodies. We directly injected anti-CRMP5 sera from four patients (diluted 1/10) into the paw of rats, allowing direct exposure of nociceptive terminals in the skin to the autoantibodies. Remarkably, hindpaw injection of CV2/CRMP5-Abs from these patients led to robust mechanical hypersensitivity (Fig. 2H), demonstrating that autoantibodies can sensitize peripheral pain responses when present in the skin. Crucially, blocking the Fab region of human anti-CRMP5 using peptides 53, 142, and 146 prevented the development of mechanical hypersensitivity for all anti-CV2 sera tested (Fig. 2I, J). Collectively, our results underscore that CV2/CRMP5-Abs-induced mechanical hypersensitivity is mediated by the binding of autoantibodies to their target protein, CRMP5.

Preclinical replication of CV2/CRMP5 autoimmune pain

After establishing that autoantibodies play a pivotal role in sensory neuron sensitization and mechanical hypersensitivity in anti-CV2/CRMP5 autoimmune neuropathy, our next goal was to determine if paraneoplastic neurological syndromes could be replicated preclinically, allowing for further mechanistic investigation and determination of potential therapeutic strategies. Interestingly, direct infusion of patient autoantibodies into animals failed to fully replicate the symptoms seen in paraneoplastic neurological syndromes[30,31]. To overcome this challenge, we adopted an alternative approach: DNA immunization[32]. By injecting a plasmid containing the CRMP5 coding sequence, we invoked muscle cells to produce the antigen, which would then be recognized by the immune system. This immunization technique activates both T and B lymphocytes[33], leading to the production of CRMP5 autoantibodies in rats (Fig. S7A).

Our peptide array analysis revealed that, akin to humans, anti-CRMP5 autoantibodies from rat serum specifically targeted two epitopes: Peptides 53 and 146 (Fig. S7B). Notably, rats immunized against CRMP5 concurrently developed bilateral mechanical hypersensitivity as their autoantibody levels increased in the serum (Figs. 3A, B and S7A). Surprisingly, we did not observe thermal hypersensitivity (Fig. 3C, D), suggesting that CRMP5 autoimmunity predominantly sensitizes mechanical responses. To further explore this link between mechanical hypersensitivity and pain, we employed the mechanical conflict-avoidance assay. In this test, rats had to navigate a field of sharp probes to escape a bright light aversive stimulus and reach a safe, dark chamber[34]. Strikingly, rats with CRMP5 autoimmunity took longer to cross the probe-filled field compared to control rats, indicating that their heightened tactile sensitivity was associated with an aversive (painful) effect (Fig. S7C). Consistent with the lack of sex differences in pain reported clinically, these findings held true for both male (Fig. 3A–D) and female rats (Fig. 3E–H).

Subsequently, we cultured male and female DRG neurons and recorded their action potential firing (Fig. 3I). Neurons from rats immunized against CRMP5 exhibited an increased frequency of evoked action potential discharge compared to control neurons (Fig. 3J). Additionally, the rheobase was lower in CRMP5-immunized rats (Fig. 3K, L). Interestingly, cultured DRG neurons from rats with CRMP5 autoimmunity released anti-CRMP5 autoantibodies in culture while still containing intracellular autoantibodies (Fig. S7D). Collectively, these results strongly suggest that primary afferent neurons become sensitized in the context of CRMP5 autoimmunity.

To further test our approach, we conducted an ex vivo assay. By applying a depolarization stimulus, we induced the release of calcitonin gene-related peptide (CGRP) from the spinal cord, which we quantified using ELISA. Remarkably, this assay demonstrated increased CGRP release in rats with autoimmunity against CRMP5, highlighting the association with pain (Fig. S7E). Rats showed no motor impairments (Fig. S8A–C) but displayed mild anxiety-like behaviors in the open-field test, consistent with their pain phenotype (Fig. S8D–G). Altogether, our findings underscore the successful use of DNA immunization to induce CRMP5 autoimmunity, faithfully recapitulating the pain symptoms and autoantibody profiles observed in patients.

Preclinical evaluation of potential therapies for CRMP5 autoimmune painful neuropathies

High-dose IV corticosteroids are commonly used to manage symptoms associated with CRMP5 autoimmunity, including pain[2]. While this therapy can be effective, it is associated with a multitude of undesired side effects. For this reason, we evaluated the efficacy of commonly used clinical therapies, including acetaminophen, ibuprofen (a non-steroidal anti-inflammatory drug), amitriptyline and duloxetine (reuptake blockers), gabapentin and morphine[35] on mechanical allodynia in rats immunized with the CRMP5 coding sequence. Since male and female rats exhibited similar behavior profiles over time, we conducted drug tests only in male rats (Fig. 3). Consistent with clinical observations[2], pain induced by CRMP5 autoimmunity was reversed by ibuprofen (100 mg/kg, p.o.), amitriptyline (50 mg/kg, p.o.) or duloxetine (30 mg/kg, p.o.) (Fig. S9A)

https://doi.org/10.1038/s41467-025-62380-y

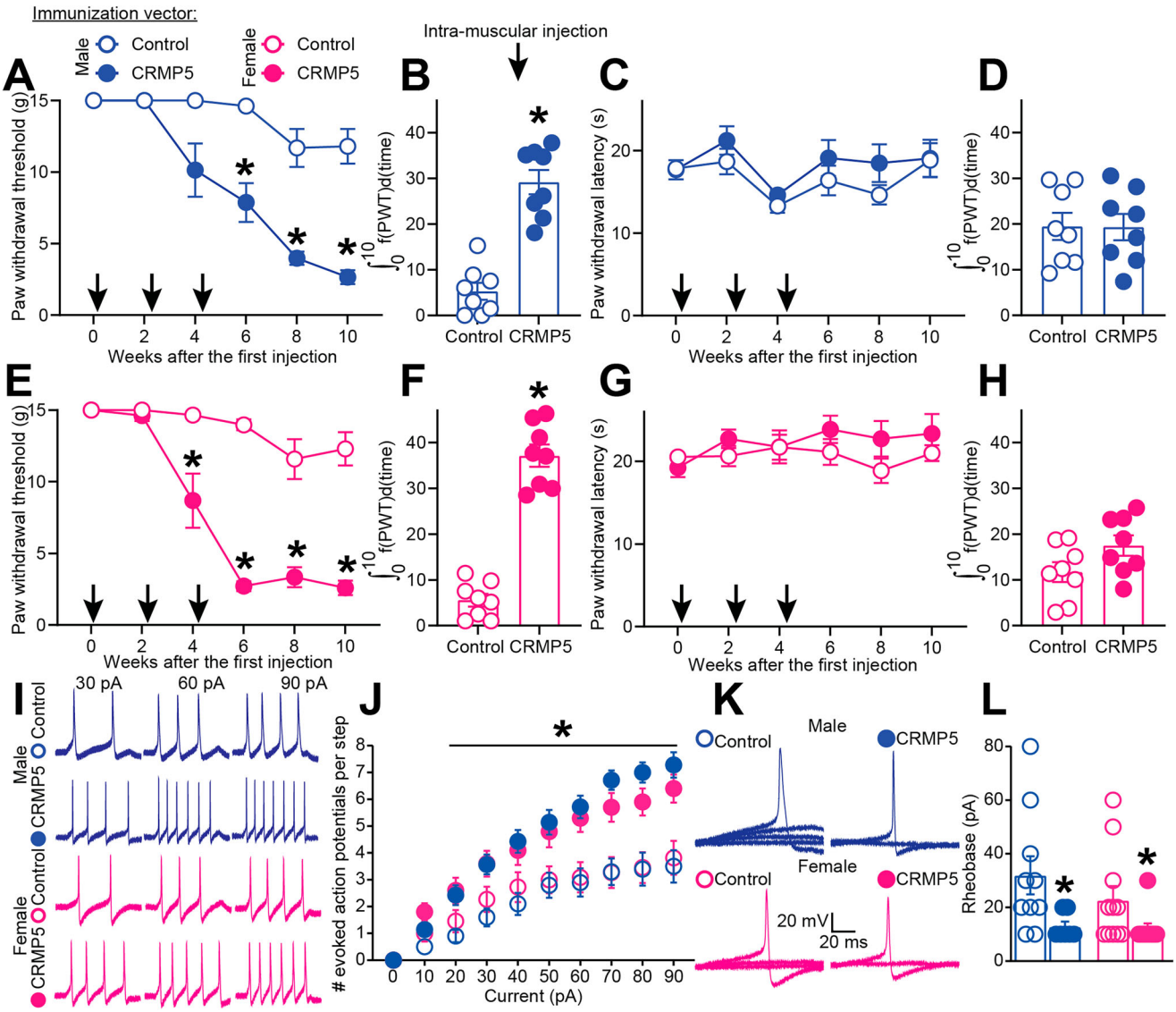

Fig. 3 | CRMP5 autoimmunity induces mechanical allodynia and hyperexcitability in both male and female rats. Rats were immunized by three injections (indicated by arrows) of 50 μg of pCMV2 plasmid, allowing for the expression of CRMP5 or control (empty) in the spinodeltoidus muscle. Rats received an intramuscular injection of a plasmid (pCMV2-CRMP5) carrying the coding sequence for CRMP5 on day 0 and then two booster shots at weeks 2 and 4 after the first injection. Graph showing the paw withdrawal threshold of **A** male and **E** female rats injected with the CRMP5 coding plasmid compared to the control empty plasmid ($n = 8$ animals per group; $^*p < 0.05$, two-way ANOVA). Bar graph with scatter plot showing the area under the curve for the mechanical thresholds in **B** male and **F** female rats injected as described above ($n = 8$ animals per group; $^*p < 0.05$, two-tailed, Mann–Whitney test). Rats were tested for their thermal thresholds using Hargreave's test, and no difference was found in **C** male and **G** female rats injected with the CRMP5 coding plasmid compared to the control empty plasmid ($n = 8$ animals per group; two-way ANOVA). Bar graph with scatter plot showing the area under the curve for the thermal thresholds in **D** male and **H** female rats injected as described above ($n = 8$ animals per group; two-tailed, Mann–Whitney test. **I** Representative recordings in response to a depolarizing current step to evoke action potentials (APs) in sensory neurons from male and female rats injected with a plasmid expressing CRMP5 or a control plasmid. **J** Summary of the number of APs in the indicated conditions. $^*p < 0.05$, multiple Mann–Whitney tests. Male control $n = 10$ cells, Male CRMP5 $n = 7$ cells, Female control $n = 11$ cells, Female control $n = 10$ cells from at least three rats. **K** Representative recordings in response to various steps of depolarizing current to measure rheobase in sensory neurons prepared from rats with CRMP5 autoimmunity or control. **L** Summary of the measured rheobase in indicated conditions. Asterisks indicate significance compared with control $^*p < 0.05$, two-tailed, Mann–Whitney test. Male control $n = 10$ cells, Male CRMP5 $n = 7$ cells, Female control $n = 11$ cells, Female control $n = 10$ cells from at least three rats. All data are shown with error bars that indicate mean ± SEM. See Supplementary Data 1 for additional statistical details. Source data are provided as a Source Data file.

but not acetaminophen (200 mg/kg, p.o.). As anticipated[2], morphine effectively alleviated mechanical hypersensitivity in rats with CRMP5 autoimmunity (Fig. S9A). Interestingly, gabapentin (30 mg/kg, p.o.) had little to no effect (Fig. S9A). Overall, amitriptyline, duloxetine, and morphine demonstrated the strongest reduction of CRMP5 autoimmunity-induced pain (Fig. S9B).

These results highlight the effectiveness of clinically used drugs in managing pain for patients with CRMP5 autoimmune neuropathy. However, these drugs typically offer short-term relief based on their pharmacokinetic profiles and do not represent long-term treatment options for this patient population. To explore a more lasting solution, we investigated the benefits of an anti-CD20 monoclonal antibody (Genentech, 4 mg/kg, i.p.[36]) for its potential as a long-term therapy to reverse pain from CRMP5 autoimmune painful neuropathy. Anti-CD20 specifically targets B lymphocytes as autoantibody-producing cells[37] and is currently used to treat conditions such as

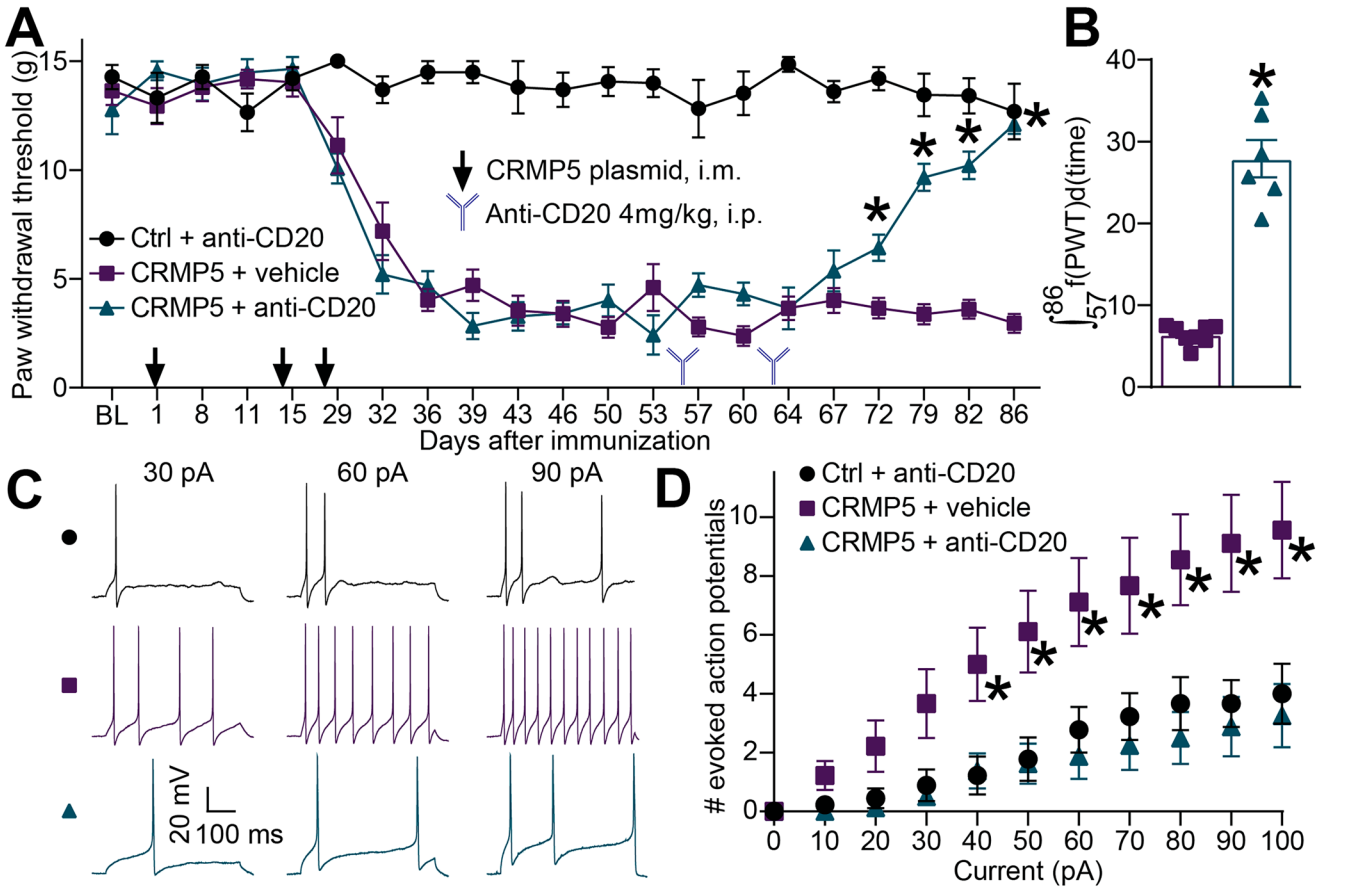

Fig. 4 | The anti-CD20 monoclonal antibody reverses CRMP5 autoimmunity-induced mechanical hypersensitivity and hyperexcitability. Male rats were immunized against CRMP5 and developed stable mechanical hypersensitivity up to day 86 after the first intramuscular injection. **A** Graph showing the paw withdrawal threshold of rats over time. Black arrows show the three plasmid injections necessary for the induction of the model. Anti-CD20 injection (4 mg/kg, i.p.) is indicated at days 56 and 63 by an antibody symbol. Control + Anti-CD20 $n = 6$, CRMP5 autoimmunity + Vehicle $n = 8$, CRMP5 autoimmunity + anti-CD20 $n = 6$, $^*p < 0.05$ two-way ANOVA. **B** Bar graph with scatter plot showing the area under the curve for each individual from the indicated treatment groups. CRMP5 autoimmunity + Vehicle $n = 8$, CRMP5 autoimmunity + anti-CD20 $n = 6$. $^*p < 0.05$, two-tailed, Mann–Whitney test. **C** Representative recordings of evoked action potentials recorded from rat small-diameter DRG neurons cultured from the indicated treatment groups in response to depolarizing current injection of 30, 60, and 90 pA. **D** Quantification of the number of current-evoked action potentials in response to 0–100 pA injected current. CRMP5 autoimmunity increased action potential firing compared to control DRG neurons. Anti-CD20 reversed this phenotype back to the level of control sensory neurons. $^*p < 0.05$, multiple Mann–Whitney tests. Control + Anti-CD20 $n = 9$ cells, CRMP5 autoimmunity + Vehicle $n = 9$ cells, CRMP5 autoimmunity + anti-CD20 $n = 8$ cells obtained from at least three rats. All data are shown with error bars that indicate mean ± SEM. See Supplementary Data 1 for additional statistical details. Source data are provided as a Source Data file.

non-Hodgkin lymphoma, chronic lymphocytic leukemia, refractory rheumatoid arthritis, and other autoimmune neurological disorders[38]. We administered anti-CD20 on day 56 and then on day 63 to rats with CRMP5 autoimmunity. The treatment effectively depleted B lymphocytes present in their serum (Fig. S10A, B) and lowered serum levels of anti-CRMP5 autoantibodies (Fig. S8C). During our injection protocol, we measured mechanical withdrawal thresholds (Fig. 4A) and observed that anti-CD20 completely reversed the mechanical hypersensitivity induced by CRMP5 autoimmunity (Fig. 4B). Since CRMP5 autoimmunity leads to hyperexcitability of DRG sensory neurons, we further investigated whether anti-CD20 could reverse this sensitization state (Fig. 4C). Remarkably, the excitability profile of DRG neurons prepared from rats with CRMP5 autoimmunity and treated with anti-CD20 was comparable to control levels (Fig. 4D). Additionally, the rheobase of neurons from anti-CD20-treated rats returned to the level of control rats (Fig. S10D, E). These findings demonstrate that anti-CD20 has the potential to fully reverse sensory neuron sensitization and pain induced by CRMP5 autoimmunity, offering hope for treating CRMP5 painful autoimmune neuropathy in humans.

Discussion

Here, we report a previously unknown role of CV2/CRMP5-Abs in autoimmune painful neuropathy experienced by patients. These autoantibodies specifically target DRG neurons and spinal cord laminae I/IIo, where nociceptive signals converge. Intrathecal or intra-paw application of sera containing these autoantibodies induces mechanical hypersensitivity in rats. At the cellular level, sensory neurons become hyperexcitable upon exposure to CV2/CRMP5-Abs. We identified epitopes on CRMP5 that are targeted by these autoantibodies and successfully masked them to reduce DRG neuron sensitization and mechanical hypersensitivity. Additionally, the painful autoimmune neurological syndrome was replicated preclinically following DNA immunization. Notably, the anti-CD20 monoclonal antibody, named Rituximab in the clinic, emerged as a promising treatment option for patients with CRMP5 autoimmune painful neuropathy. Overall, the data strongly suggest that pain symptoms in anti-CV2/CRMP5 patients result from autoimmunoreactivity with DRG neurons, which can be effectively managed with anti-CD20.

This study stems from the remarkable clinical observation that ~80% of patients with CV2/CRMP5-Abs exhibit painful neuropathy[2].

The prevalence of pain in a rare disease surpasses what is typically reported in common pain conditions, including diabetic neuropathy (42%)[6] and chemotherapy-induced neuropathy (60%)[8]. Pain management for CV2/CRMP5-Abs patients necessitates at least two pain medications, with opioids being used in 39% of cases[2]. Notably, evidence suggests that pain in anti-CRMP5 patients can be alleviated by reducing antibody levels[2]. These findings strongly implicate the autoantibodies as direct contributors to heightened pain sensation in patients. To investigate this, we employed two approaches to directly assess whether CV2/CRMP5-Abs could enhance pain sensitivity: (1) we removed CV2/CRMP5-Abs from patient sera through adsorption on a purified CRMP5 substrate, and (2) we targeted the Fab regions of human autoantibodies using peptides that mask the epitopes on CRMP5. Both approaches effectively neutralized the functional impact of CV2/CRMP5-Abs on DRG neuron excitability and pain. Intriguingly, CV2/CRMP5-Abs induced mechanical allodynia, whether applied directly to the spinal cord or injected into the hindpaw. These findings suggest that CV2/CRMP5 autoantibodies can target sensory neurons at both peripheral and central levels, potentially explaining their clinical association with painful, asymmetric polyradiculoneuropathies. These findings lead us to conclude that CV2/CRMP5-Abs are pathogenic and that therapies aimed at reducing autoantibody levels in patients hold promise for mitigating their pain symptoms.

The autoantigen target of CV2/CRMP5-Abs, CRMP5, is a cytosolic protein[11,39]. While these autoantibodies can recognize a cytoplasmic antigen in fixed DRG and spinal cord tissues[15], their ability to access the cytosolic CRMP5 protein under physiological conditions remains uncertain. Previous reports have demonstrated that autoantibodies can penetrate cells to bind to intracellular targets, even in the case of nuclear antigens (e.g., anti-Hu, Sm, or La)[40–42]. In a separate study involving rats, peripherally injected rabbit IgG was transported into neurons within the spinal cord, further illustrating that antibodies can penetrate neuronal cytoplasm in vivo[43]. A post-mortem study in patients with paraneoplastic syndrome revealed positive immunofluorescence for circulating autoantibodies in Purkinje and DRG neurons[44]. Specifically concerning DRG neurons, studies have suggested that following immunization in rats, antibodies were sequestered and retained within their soma[45]. These intriguing findings raise the possibility that sensory neurons are a vulnerable target of autoantibodies targeting neuronal antigens, emphasizing the intricate relationship between the immune and nervous systems. While we cannot fully exclude an extracellular action of CV2/CRMP5-Abs, our results support the hypothesis that the elevated prevalence of pain in autoimmune diseases, such as anti-CV2/CRMP5 autoimmune encephalitis, may be linked to the intracellular retention of autoantibodies in sensory neurons, ultimately contributing to pain sensitization. This hypothesis will require further exploration.

We demonstrated that CV2/CRMP5-Abs can bind their target in DRG sensory neurons to induce hyperexcitability and pain. Although CRMP5 has not previously been linked to pain, these data suggest that it may play a role in sensory neuron function. Another member of the CRMP family, CRMP2, has been extensively described to be phosphorylated and SUMOylated in chronic pain to increase the function of voltage-gated ion channels NaV1.7 and CaV2.2, supporting hyperexcitability[22,46–50]. During neuronal polarization, CRMP5 is known to antagonize CRMP2 function, promoting microtubule polymerization[13]. The exact role of CRMP5 expression in sensory neurons remains to be elucidated. By analogy with CRMP2[22,46–50], CRMP5 is likely to be involved in ion channel trafficking and restricting neuronal excitability. CV2/CRMP5-Abs would block the action of CRMP5, thereby allowing facilitated action potential firing in sensory neurons.

Our comprehensive investigations using calcium imaging and electrophysiology revealed that CV2/CRMP5-Abs exert a specific impact on sensory neuron function. Constellation pharmacology ruled out the possibility that heightened sensitivity to heat, cold, itch, or inflammation by DRG neurons could account for pain in patients with these autoantibodies. Instead, we found that DRG neurons exposed to CV2/CRMP5-Abs exhibited increased action potential firing and decreased rheobase. This suggests that CV2/CRMP5-Abs have a dual impact: lowering the threshold for firing and increasing the number of action potentials generated in response to stimuli. Notably, we correlated excitability with mechanical hypersensitivity throughout our experiments. Hyperexcitability, a hallmark of neuropathic pain observed in both rodent models and patients[24,25], implies that pain symptoms in individuals with CV2/CRMP5-Abs may be more amenable to drugs aimed at reducing neuronal activity. In the absence of clinically available drugs aimed at silencing sensory neurons, our screening campaign revealed enhanced benefits from amitriptyline and duloxetine in reversing CRMP5 autoimmunity-induced mechanical hypersensitivity. Although CRMP5 is broadly expressed across DRG neurons, the reason why CV2/CRMP5-Abs selectively elicit mechanical hypersensitivity remains unclear but likely reflects modality-specific vulnerability.

Limitations of our study include the restricted and variable availability of CV2/CRMP5-Abs positive sera in the biobank. Consequently, we were unable to systematically test all patients' sera in all our experiments. Another limitation is that our sample set predates the implementation of systemic classification of pain symptoms by the International Classification of Diseases-11, and therefore reports of pain symptoms might not reflect current practices. Additionally, it is uncertain if our collection might exhibit bias on the basis of patient sex, though sex-based prevalence associated with the development of CV2/CRMP5-Abs has not been reported[2,15]. Despite these limitations, our epitope profiling revealed that all samples identified similar epitopes on CRMP5, suggesting equivalence from this perspective. We opted not to factor in the titer of autoantibodies in our samples, as previous research has not consistently linked these levels to the severity of patient symptoms. Our strategies for depleting autoantibodies or blocking the Fab domain demonstrated that other serum components had limited impact on our pain and excitability studies, reinforcing the pathological role of CV2/CRMP5-Abs. Our findings with human sera align with data showing that depleting B lymphocytes using the anti-CD20 monoclonal antibody Rituximab could serve as a long-term treatment for CRMP5 autoimmune painful neuropathy. Notably, patients with anti-CV2/CRMP5 autoimmunity are often diagnosed with cancer. Treatment with anti-CD20 bears the potential to synergize with classical chemotherapeutics[37], which could help with the elimination of primary tumors in addition to relieving autoimmune pain. Still, careful consideration should be given to determine if the benefits outweigh the risks of such treatment[38]. B lymphocyte repopulation typically occurs within 6–9 months following anti-CD20 therapy[51], and Rituximab is generally well tolerated with no significant toxicities reported[52]. In an open-label study of patients with rheumatoid arthritis, Rituximab treatment was not associated with an increased risk of infections, including viral airway infections[53], suggesting it may be safely administered with appropriate monitoring. Furthermore, pain is a significant comorbidity in cancer patients, and addressing pain in anti-CV2/CRMP5 patients can profoundly impact their quality of life and survival post-cancer diagnosis.

This first of its kind study directly assessing the function of an autoantibody targeting an intracellular protein. We demonstrate that CV2/CRMP5-Abs are drivers of hypersensitivity to mechanical stimuli and hyperexcitability in DRG neurons. We replicated CRMP5 autoimmunity in rats, which provided a unique preclinical platform for investigating future treatment options to relieve pain in patients. Our work identifies clinically used painkillers with a superior ability to alleviate pain in patients with CV2/CRMP5-Abs. We propose a novel therapeutic approach by repurposing anti-CD20 monoclonal antibodies to treat pain long-term in patients with CRMP5 autoimmunity.

Methods

Patients

Sera used in this study were collected as part of the standard diagnostic procedures in the French reference center on paraneoplastic neurological diseases and then stored for research purposes as part of the Neurobiotec biobank in Lyon, France. De-identified samples with informed consent in writing from the patients were transferred to the laboratory overnight via FedEx. Research using human sera without patient personal information was performed under an Institutional Review Board exemption 4 at the University of Arizona and at Saint Louis University.

Animals

Adult Sprague-Dawley rats (Pathogen-free male and female, 100–250 g, Envigo, Placentia, CA, Order Code #002) were kept in light (12-h light: 12-h dark cycle; lights on at 07:00 h) and temperature (23 ± 3 °C) controlled rooms. Standard rodent chow and water were available *ad libitum*. All animal use was conducted in accordance with the National Institutes of Health guidelines and with recommendations in the Guide for the Care and Use of Laboratory Animals. All animal studies were approved by the Institutional Animal Care and Use Committee of Saint Louis University (Protocol #: 3014) and the University of Arizona and housed in a specified pathogen-free facility. All behavioral experiments were performed by experimenters who were blinded to treatment groups, and animals were randomly assigned to treatment groups. Animals from experimental and control groups were housed in separate cages within the same room of the facility.

Human dorsal root ganglia

Human DRG were obtained from Mid-America Transplant at St. Louis University within an hour of cross-clamping and immediately picked up and processed by laboratory personnel. All studies involving human tissues have been classified for an IRB exemption #4 at Saint Louis University. DRGs from one female donor were fixed by immersion in 10% formalin for at least 1 day. After fixation, the DRGs were trimmed of their connective tissue and roots, cut in half, prior to embedding into paraffin blocks. The paraffin blocks were sectioned into 5 μm slices. Deparaffination is carried out by three xylene washes for 5 min each, followed by two 100% alcohol washes for 1 min each, then two 95% alcohol washes for 1 min each, and finally by washing in running water for 2 min. For antibody staining, the slides were washed twice with phosphate buffered saline (PBS) for 5 min each at room temperature (RT), then exposed for 30 min to a blocking solution containing 5% donkey serum (Cat# ab138579, Abcam) and 1% BSA (Cat# A-420, Goldbio) in PBS at RT. The primary antibody against CRMP5 (1:100, from ref. 20) was then incubated in blocking buffer overnight at 4 °C in a humidified chamber. The slides were then washed 3 times, 15 min with PBS at RT before adding the secondary antibody solution (donkey anti-rabbit, Alexa Fluor 488, 1/300, Cat#A-21206, Thermo Fisher Scientific) for 1 h at RT. Slides were then washed with PBS 3 times for 15 min at RT. Finally, slides were mounted in ProLong Gold (Cat# P36930, Thermo Fisher Scientific) to protect from fading and photobleaching. To evaluate the background due to the secondary antibody alone, the primary antibody was omitted. Immunofluorescent micrographs were acquired on a Leica SP8 inverted microscope using a 10× dry objective. The freeware image analysis program Image J was used for extracting representative pictures after contrast enhancement for better visualization.

Materials and reagents

All peptides (98% purity) were purchased from Genscript (Piscataway, NJ). All chemicals, unless noted, were purchased from Sigma (St. Louis, MO). Fura-2 AM (Cat# F1221, Life Technologies) was obtained from Life Technologies. Subcellular proteome extraction kit (Cat# 539790, Millipore). Antibodies used are as follows: CRMP5 from ref. 20, Goat anti-Human IgG Cross-Adsorbed, Alexa Fluor 488 (Cat# A11013, Life Technologies), Goat anti-Rabbit IgG, Alexa Fluor 555 (Cat# A21429, Life Technologies), Rabbit anti-Human IgG DyLight 800 (Cat# SA5-10116, Thermo Fisher). For the appraisal of common painkillers drugs were as follows: ibuprofen (100 mg/kg, Cat# I4883, Sigma), acetaminophen (200 mg/kg, Cat# A3035, Sigma), gabapentin (100 mg/kg, Cat# G154, Sigma), amitriptyline (50 mg/kg, Cat# A8404, Sigma), duloxetine (30 mg/kg, Cat# SML0474, Sigma) and morphine (10 mg/kg, Cat# M8777, Sigma). The selected medication doses were determined from previously documented animal studies, and we opted for oral administration as it is the predominant method utilized in clinical settings[54–58].

Purification of CRMP5-GST

CRMP5-GST fusion protein was purified similarly to a previously described protocol (François-Moutal et al.[59]). BL21 *Escherichia coli* cells (Cat# C2527H, New England Biolabs, Ipswich, MA) expressing recombinant CRMP5-GST were resuspended in 50 mM HEPES, pH 7.5, 500 mM NaCl, 10% glycerol (vol./vol), 0.5 mM Tris(2-carboxyethyl) phosphine hydrochloride (TCEP), supplemented with complete EDTA-free protease inhibitors (Roche, Basel, Switzerland). Disruption of the bacteria was performed by sonication, and the lysate was centrifuged at 4 °C for 45 min at 20,000 × *g*. The supernatant was loaded on a GST-Trap HP column (Cat# 17528201, Cytiva, Marlborough, MA) equilibrated with 50 mM HEPES pH 7.5, 500 mM NaCl, 10% glycerol, 0.5 mM TCEP. After a washing step with 50 mM HEPES, pH 7.5, 5 mM Glutathione, 500 mM NaCl, 10% glycerol, 0.5 mM TCEP, CRMP5-GST was eluted with a step gradient up to 40 mM Glutathione. The eluted protein was concentrated with Amicon Ultra 15 centrifugal filters (Regenerated cellulose 10,000 NMWL; Merck Millipore, Darmstadt, Germany), aliquoted, and flash-frozen on dry ice and stored at −80 °C until use. Protein concentration was determined by a Pierce assay using BSA as a standard. The purity of the protein was verified with SDS-PAGE.

Immunohistochemistry

Freshly prepared adult rat spinal cord was fixed in 4% paraformaldehyde (EM-15713-S, Euromedex, Sousselweyrsheim, France) for 1 h, frozen, and sliced into 10 μm-thick sections. Tissue was permeabilized and blocked for 1 h at RT in a blocking buffer containing PBS supplemented with 5% (v/v) normal goat serum, 2% (m/v) bovine serum albumin, and 0.25% (v/v) Triton X-100. Double immunolabeling was performed using patient serum (1:100) and rabbit anti-CRMP5 antibody (1:400[20]) in blocking buffer for 2 h at RT. Tissue was washed 3 times 10 min, at RT with 1 ml of PBS, and revealed with appropriate Alexa fluorophore-conjugated secondary antibodies (1:1000 in blocking buffer, A11013 and A21429, Thermo Fisher, Courtaboeuf, France) and DAPI (Cat# D1306, Thermo Fisher Scientific, 10 μg/mL) for 1 h at RT. Photos of immunolabeling were acquired on Axio Scan.Z1 (Carl Zeiss SAS, Rueil Malmaison, France) with 20×, 0.8 NA, Plan-Apochromat objective (Carl Zeiss SAS, Rueil Malmaison, France). Images were visualized and analyzed by means of ZEN (Blue) software (Carl Zeiss SAS, Rueil Malmaison, France) and ImageJ.

Proximity ligation assay

PLA was performed to visualize the close proximity (less than 30 nm) between the human anti-CV2 autoantibodies and their target CRMP5 in cultured DRG neurons. DRG neurons were incubated overnight with the indicated sera diluted 1:100 before fixation using 4% paraformaldehyde for 20 min at RT. Blocking and permeabilization were done by incubating the cells with PBS, 0.1% Triton X-100, with 3% BSA for 30 min at RT. Fixed DRG neurons were incubated with anti-CRMP5 antibody for 1 h at RT in PBS, 0.1% Triton X-100, 3% BSA before 3 washes in PBS, 0.1% Triton for 5 min at RT. The proximity ligation reaction and visualization of signal were performed according to the

manufacturer's protocol using the Duolink Detection Kit with PLA PLUS and MINUS probes for rabbit and human antibodies (Cat# DUO92020, Cat# DUO92005, Sigma). DAPI stain was used to detect cell nuclei. Immunofluorescent micrographs were acquired on a Nikon Eclipse Ti/U microscope with a Photometrics cooled CCD camera, CoolSNAP ES2 (Roper Scientific, Planegg, Germany), controlled by NIS Elements software (version 4.20, Nikon Instruments), using a 60X plan Apo 1.40 numerical aperture objective.

Enzyme-linked immunosorbent assay-based CRMP5-anti-CV2 binding assay

96-well plates (Nunc MaxiSorp, Thermo Scientific) were coated with CRMP5-GST (200 ng per well) and incubated at RT overnight. The next day, the plates were washed and blocked with 3% BSA to minimize nonspecific adsorptive binding to the plates. The plates were incubated at RT with serum from patients (diluted 1:100 in PBS) with the indicated peptide at 100 ng/ml and left on gentle shaking for 2 h. The plates were then washed with PBS containing 0.5% Tween 20. The bound anti-CV2 was detected by HRP-conjugated secondary antibody (Cat# 309-035-064, Jackson Immunoresearch). Tetramethylbenzidine (Cat# DY999, R&D Systems) was used as the colorimetric substrate. The optical density of each well was determined immediately, using a microplate reader (Multiskan Ascent, Thermo) set to 450 nm with a correction wavelength of 570 nm.

Peptide synthesis and spotting on a peptide array

Standard 9-fluorenylmethoxy carbonyl (Fmoc) chemistry was used to synthesize the peptides and spot them onto Celluspots nitrocellulose disks prederivatized with a polyethylene glycerol spacer (Cat# 32121, Intavis). Peptide synthesis was done using the Respep peptide synthesizer using established protocols from Intavis. After synthesis, a side chain deprotection step was done in 80% trifluoroacetic acid (TFA, Cat# 302031, Sigma), 3% triisopropylsilane (TIPS, Cat# 8413590010, Sigma), 12% dichloromethane (DCM, Cat# 34856, Sigma), 5% H_2O for 2 h at RT. Next, the Celluspots were solubilized in 88.5% TFA, 4% trifluoromethanesulfonic acid (TFMSA, Cat# 8211660025, Sigma), 2.5% TIPS, 5% H_2O overnight at RT before precipitation by adding 4:1 ice-cold tert-butyl-methyl ether (Cat# 34875, Sigma). Cellulose-peptide conjugates were pelleted by a 5000 × *g*, 10 min, 0 °C centrifugation step. After removing the supernatant, the pellets were allowed to dry until achieving a gel-like texture at RT and resuspended in 100% DMSO (Cat# 34869, Sigma). The peptides were spotted on 20 membranes fitted on glass microscope slides (Cat# 54112, Intavis) using an Intavis MultiPep robot. All chemicals were HPLC grade and obtained from Sigma.

Hybridization and immunoblotting of peptide arrays

Celluspots slides were washed in TBST (50 mM Tris-HCl, pH 7.4, 150 mM NaCl, 0.1% Tween 20) for 10 min, 5% (mass/vol) non-fat dry milk, and then blocked for 1 h at RT with gentle shaking in TBST containing 5% (w/v) non-fat dry milk. Sera were diluted 100 times in TBST, 5% non-fat dry milk, and incubated on the slide overnight. Peptide arrays were washed 3 times for 5 min at RT with TBST and incubated with the antibody Rabbit anti-Human IgG DyLight 800 (Cat# SA5-10116, Thermo Fisher, 1/1000) diluted in TBST, 5% BSA for 2 h at RT. The arrays were washed 3 times, 5 min in TBST, and visualized by infrared fluorescence. All arrays contained quadruplicates that were averaged and then normalized to the maximum signal on the array for each patient.

Acute dissociation and culture of dorsal root ganglia (DRG) neurons

DRG were dissected from Sprague-Dawley rats. Rats were anesthetized with isoflurane, followed by rapid decapitation with a guillotine. In brief, removing dorsal skin and muscle and cutting the vertebral processes parallel to the dissection stage exposed DRGs. DRGs were then collected, trimmed at their roots, and digested in 3 ml bicarbonate free, serum free, sterile DMEM (Cat# 11965, Thermo Fisher Scientific, Waltham, MA) solution containing neutral protease (3.125 mg/ml, Cat# LS02104, Worthington, Lakewood, NJ) and collagenase Type I (5 mg/ml, Cat# LS004194, Worthington, Lakewood, NJ) and incubated for 45 min at 37 °C under gentile agitation. Dissociated DRG neurons (~1.5×10^6) were then gently centrifuged to collect cells and washed with DRG DMEM media containing 1% penicillin/streptomycin sulfate from 10,000 μg/ml stock, 30 ng/ml nerve growth factor (Cat# N2513, Sigma Aldrich), and 10% fetal bovine serum (Cat# 25-550, Genesee). Cells were plated onto poly-D-lysine (Cat# 34392000101, Fisher Scientific)—and laminin-coated (Cat# 23017015, Fisher Scientific) glass 12- or 15-mm coverslips (Cat# 76305-514, VWR). For rat DRG culture, small cells were considered to be approximately <30 μm diameter in size. All cultures were used within 48 h.

Calcium imaging

DRG neurons were loaded at 37 °C with 3 μM Fura-2 AM (Cat#F-1221, Life technologies, stock solution prepared at 1 mM in DMSO, 0.02% pluronic acid, Cat# P-3000MP, Life technologies) for 30 min (K_d = 25 μM, λ_{ex} 340, 380 nm/λ_{emi} 512 nm) to follow changes in intracellular calcium ($[Ca^{2+}]_c$) in Tyrode's solution (at ~310 mOsm) containing 119 mM NaCl, 2.5 mM KCl, 2 mM $MgCl_2$, 2 mM $CaCl_2$, 25 mM HEPES, pH 7.4 and 30 mM glucose. All calcium-imaging experiments were done at RT (~23 °C). Baseline was acquired for 1 min followed by stimulation (15 s) with an excitatory solution (at ~310 mOsm) comprised of 32 mM NaCl, 90 mM KCl, 2 mM $MgCl_2$, 2 mM $CaCl_2$, 25 mM HEPES, pH 7.4 and 30 mM glucose. Fluorescence imaging was performed with an inverted microscope, Nikon Eclipse T*i*-U (Nikon Instruments Inc.), using a Nikon Super Fluor MTB FLUOR 10× 0.50 NA objective and a Photometrics cooled CCD camera CoolSNAP ES^2 (Roper Scientific) controlled by NIS Elements software (version 4.20, Nikon Instruments). The excitation light was delivered by a Lambda-LS system (Sutter Instruments). The excitation filters (340 ± 5 nm and 380 ± 7 nm) were controlled by a Lambda 10-2 optical filter changer (Sutter Instruments). Fluorescence was recorded through a 505 nm dichroic mirror at 535 ± 25 nm. To minimize photobleaching and phototoxicity, the images were taken every 10 s during the time course of the experiment using the minimal exposure time that provided acceptable image quality. The changes in $[Ca^{2+}]_c$ were monitored by following the ratio of F_{340}/F_{380}, calculated after subtracting the background from both channels.

Constellation pharmacology

DRG neurons were loaded at 37 °C with 3 μM Fura-2 AM for 30 min in Tyrode's solution. After a 1-min baseline measurement Ca^{2+} influx was stimulated by the addition of the following receptor agonists: 400 nM menthol, 50 μM histamine, 10 μM adenosine triphosphate (ATP), 200 μM allyl isothiocyanate (AITC), 1 mM acetylcholine (Ach), 100 nM capsaicin diluted in Tyrode's solution. At the end of the constellation pharmacology protocol, cell viability was assessed by depolarization-induced Ca^{2+} influx using an excitatory KCl solution comprised of 32 mM NaCl, 90 mM KCl, 2 mM $MgCl_2$, 2 mM $CaCl_2$, 25 mM HEPES, pH 7.4, 30 mM glucose. After the 1-min baseline measurement, each trigger was applied for 15-s in the order indicated above in 6-min intervals. Following each trigger, the bath solution was continuously perfused over the cells to wash off excess trigger solution. Fluorescence imaging was performed under the same conditions noted above for calcium imaging. A cell was defined as a "responder" if its fluorescence ratio of 340 nm/380 nm was greater than 10% of the baseline value calculated using the average fluorescence in the 30 s preceding application of the trigger.

Measurement of action potentials using whole-cell current-clamp electrophysiology

Patch-clamp recordings were performed at RT (22–24 °C). For current-clamp recordings, the external solution contained (in millimolar): 154 NaCl, 5.6 KCl, 2 $CaCl_2$, 1 $MgCl_2$, 10 D-Glucose, and 8 HEPES (pH 7.4 adjusted with NaOH, and mOsm/L = 300). The internal solution was composed of (in millimolar): 137 KCl, 10 NaCl, 1 $MgCl_2$, 1 EGTA, and 10 HEPES (pH 7.3 adjusted with KOH, and mOsm/L = 277). At RT (22–24 °C), a tight seal with the cell membrane was established by applying negative pressure to obtain a seal resistance >1 GΩ. A brief pulse of negative pressure was then applied to rupture the cell membrane and establish the whole-cell patch clamp configuration. Neurons were initially held at −60 mV in voltage clamp mode to measure seal quality before switching to current-clamp mode, where the current injection was immediately set to 0 pA to measure the resting membrane potential (RMP). DRG neurons with an RMP more hyperpolarized than −40 mV, stable baseline recordings, and evoked spikes that overshot 0 mV were used for experiments and analysis. Action potentials were evoked by current injection steps from 0–120 pA with an increment of 10 pA in 300 ms. Rheobase was measured by injecting currents from 0 pA with an increment of 10 pA in 50 ms.

Pipettes were pulled from standard wall borosilicate glass capillaries (Sutter Instruments) with a horizontal puller (Model P-97, Sutter Instruments). The resistance of the pipettes when filled with internal solution and immersed in the recording bath ranged from 2 to 4 MΩ. Recordings were performed from small DRG neurons with capacitance between 10 and 35 pF (~18–33 µm). Series resistance under 7 MΩ was deemed acceptable. All experiments had a series resistance compensation between 60–90%. Signals were filtered at 10 kHz and digitized at 10–20 kHz. Analyses were performed using Fitmaster software (HEKA) and Origin 9.0 software (OriginLab).

Indwelling intrathecal catheter

Rats were anesthetized (ketamine/xylazine anesthesia, 80/12 mg/kg i.p., Cat# K113, Sigma) and placed in a stereotaxic apparatus. The cisterna magna was exposed and incised, and an 8 cm catheter (PE-10, Cat# 51150, Stoelting) was implanted and terminated in the lumbar region of the spinal cord[60]. Catheters were sutured (3-0 silk suture) into the deep muscle and externalized at the back of the neck; skin was closed with autoclips, and behavioral evaluations were performed after a 5–7-day recovery period. Rats were injected with the indicated serum or their IgG-depleted counterparts. IgG depletion was achieved using protein G dynabeads (Cat# 10004D, Thermo Fisher) incubated with the whole serum for 2 h at 4 °C. Protein G dynabeads captured all the IgG in the serum, and the supernatant was considered depleted of IgGs.

Testing of allodynia

The assessment of tactile allodynia (i.e., a decreased threshold to paw withdrawal after probing with normally innocuous mechanical stimuli) consisted of testing the withdrawal threshold of the paw in response to probing with a series of calibrated fine (von Frey) filaments. Each filament was applied perpendicularly to the plantar surface of the paw of rats held in suspended wire mesh cages. The withdrawal threshold was determined by sequentially increasing and decreasing the stimulus strength (the "up and down" method), and data were analyzed with the nonparametric method of Dixon, by Chaplan et al.[61] and expressed as the mean withdrawal threshold.

Measurement of thermal withdrawal latency

The method of Hargreaves et al.[62] was used to evaluate thermal sensitivity. Rats were acclimated within Plexiglas enclosures on a clear glass plate maintained at 23 °C. A radiant heat source (high-intensity projector lamp) was focused onto the plantar surface of the hindpaw. When the paw was withdrawn, a motion detector halted the stimulus and a timer. A maximal cut-off of 33.5 s was used to prevent tissue damage.

Mechanical conflict-avoidance (MCA) assay

Voluntary mechanical conflict-avoidance was measured using the Coy mechanical conflict-avoidance system[34]. The MCA apparatus is made of a dark (safe) chamber, a sharp probe field, and a bright (~4800 lux, aversive/unsafe) chamber. The bright light serves as an aversive stimulus signaling an unsafe environment for rats. Rats have to cross a field of sharp probes (height 3 mm) to reach the safe dark area. Rats are placed in the bright compartment with the light turned off and the escape door closed. Following 15-s of dark acclimation, the compartment light is turned on for the duration of the test. The escape door is opened 20-s thereafter. Time to cross the probe bed is recorded using a stopwatch starting from the time the escape door opens. The cut-off time for this experiment was 3 min.

Genetic immunization of rats to induce CRMP5 autoimmunity

We chose to use DNA immunization[32,63] as a means to induce an immune response via both T and B lymphocytes[63–66]. Another benefit of this approach is that the methylated CpG-rich domains carried by the plasmid act as adjuvants to activate dendritic cells, leading to local production of cytokines, including interleukin (IL)-6, IL-12, and tumor necrosis factor-α, and increasing immune cell recruitment at the immunization site[67]. Rats received a unilateral intramuscular in the spinodeltoidus muscle containing 50 µg of plasmid DNA (either empty pCMV2-Flag or pCMV2-CRMP5-Flag[39] in 200 µl of saline)[68]. This was followed by two booster injections administered 2 weeks (booster 1) and 4 weeks (booster 2) after the first injection.

Ex vivo calcitonin gene-related peptide (CGRP) release from lumbar spinal cord

Rats were deeply anesthetized with 5% isoflurane and then decapitated. Two vertebral incisions (cervical and lumbar) were made to expose the spinal cord. Pressure was applied to a saline-filled syringe inserted into the lumbar vertebral foramen, and the spinal cord was extracted. Only the lumbar region of the spinal cord was used for the CGRP release assay. Baseline treatments (#1 and #2) involved bathing the spinal cord in Tyrode's solution. The excitatory solution consisting of 90 mM KCl (#3) was used to evoke CGRP release from the spinal primary afferents. These fractions (10 min, 400 µL each) were collected for measurement of CGRP release. Samples were immediately flash frozen and stored in a −20 °C freezer. The concentration of CGRP released into the buffer was measured by enzyme-linked immunosorbent assay (Cat# 589001, Cayman Chemical, Ann Arbor, MI).

Assessment of motor coordination with the Rotarod assay

Rats were trained to walk on a rotating rod (5, 10, and 15 rpm with 5 min between trials, Rotarod, Bioseb) for 1 min at a time, 3 days in a row. Training was initiated by placing the rats on a rotating rod and allowing them to walk on the rotating rod until they either fell off or 60 s had elapsed. Rats were allowed to recover for 24 h before beginning the treatment session. Assessment consisted of placing the rats on the moving rod with an increasing speed from 4 to 40 rpm over 5 min. Time to fall off the rod was recorded as well as the speed of the rotarod at the time of falling. Testing was done in a dedicated room, 3 ± 1 Lux from faerie lights, 23 °C, with the apparatus cleaned between each rat. The experimenter was blinded to treatment groups.

Open-field test

Rats were placed in an open-field square box (60 cm) and allowed to behave freely for 5 min. Rats' movements were video-tracked using the Any-MAZE software (Stoelting). Distance traveled, total time spent in each area, frequency of entries in the periphery (10 cm area on the sides of the box) and central zone (40 cm square in the center), and velocity were analyzed. Testing was done in a dedicated room, 9 ± 1 Lux from a red light, at 23 °C, with the apparatus cleaned between each rat. The experimenter was blinded to treatment groups.

Fluorescence-activated cell sorting to detect B lymphocytes in rat blood

Blood was collected from the tail vein of rats, and red blood cells were lysed in 158 mM NH_4Cl for 5 min. Lysis was quenched with PBS prior to centrifugation at 310 × *g* to pellet intact cells. This process was repeated once, and then cells were resuspended in the antibody solution containing APC anti-rat CD45RA (Cat# 202313, Biolegend) and FITC anti-rat CD3 (Cat# 201403, Biolegend) diluted 1:100 in PBS with 2% FBS for 30 min at RT. Samples were washed 3 times with PBS for 5 min and spun at 310 × *g* in between washes. Controls were made by omission of either or both antibodies. Cells were analyzed by the Flow Cytometry Research Core Facility at Saint Louis University.

Statistical methods and data analysis

Graphing and statistical analysis were undertaken with GraphPad Prism (Version 9). All data sets were checked for normality using the D'Agostino & Pearson test. Details of statistical tests, significance, and sample sizes are reported in the appropriate figure legends and in Supplementary Data 1. All data plotted represent mean ± SEM. For electrophysiological recordings: data were compared using Mann–Whitney tests (rheobase), One-way ANOVA with the Tukey post hoc test, and Kruskal–Wallis test with Dunnett's post hoc comparisons; for sensory neuron excitability, statistical differences between groups were determined using multiple Mann–Whitney tests and the Mann–Whitney test. Correction for multiple comparisons was performed using the two-stage step-up procedure of Benjamini, Krieger, and Yekutieli. All two-group comparisons are reported as two-tailed p-values. Statistical significance of hypersensitivity was compared by the Kruskal–Wallis test, followed by the Dunn post hoc test. Behavioral data with a time course were analyzed by two-way ANOVA. We used the ROUT method to determine whether data met the requirements for exclusion.

Reporting summary

Further information on research design is available in the Nature Portfolio Reporting Summary linked to this article.

Data availability

All data are included in the manuscript, the Supplementary Information, or are available from the authors, as are unique reagents used in this Article. The raw numbers for charts and graphs are available in the Source Data file whenever possible, and Source data are provided with this paper.

References

1. Graus, F. et al. A clinical approach to diagnosis of autoimmune encephalitis. *Lancet Neurol.* **15**, 391–404 (2016).
2. Dubey, D. et al. Autoimmune CRMP5 neuropathy phenotype and outcome defined from 105 cases. *Neurology* **90**, e103–e110 (2018).
3. Dubey, D. et al. Amphiphysin-IgG autoimmune neuropathy: a recognizable clinicopathologic syndrome. *Neurology* **93**, e1873–e1880 (2019).
4. Antoine, J. C. et al. Paraneoplastic anti-CV2 antibodies react with peripheral nerve and are associated with a mixed axonal and demyelinating peripheral neuropathy. *Ann. Neurol.* **49**, 214–221 (2001).
5. Honnorat, J. et al. Ulip/CRMP proteins are recognized by autoantibodies in paraneoplastic neurological syndromes. *Eur. J. Neurosci.* **11**, 4226–4232 (1999).
6. Ismail-Beigi, F. et al. Effect of intensive treatment of hyperglycaemia on microvascular outcomes in type 2 diabetes: an analysis of the ACCORD randomised trial. *Lancet* **376**, 419–430 (2010).
7. Kongkriangkai, A. M. et al. Substantial pain burden in frequency, intensity, interference and chronicity among children and adults with neurofibromatosis Type 1. *Am. J. Med. Genet. A* **179**, 602–607 (2019).
8. Seretny, M. et al. Incidence, prevalence, and predictors of chemotherapy-induced peripheral neuropathy: a systematic review and meta-analysis. *Pain* **155**, 2461–2470 (2014).
9. Charrier, E. et al. Collapsin response mediator proteins (CRMPs): involvement in nervous system development and adult neurodegenerative disorders. *Mol. Neurobiol.* **28**, 51–64 (2003).
10. Fukada, M. et al. Molecular characterization of CRMP5, a novel member of the collapsin response mediator protein family. *J. Biol. Chem.* **275**, 37957–37965 (2000).
11. Ricard, D. et al. Isolation and expression pattern of human Unc-33-like phosphoprotein 6/collapsin response mediator protein 5 (Ulip6/CRMP5): coexistence with Ulip2/CRMP2 in Sema3a- sensitive oligodendrocytes. *J. Neurosci.* **21**, 7203–7214 (2001).
12. Yamashita, N. et al. CRMP5 (collapsin response mediator protein 5) regulates dendritic development and synaptic plasticity in the cerebellar Purkinje cells. *J. Neurosci.* **31**, 1773–1779 (2011).
13. Brot, S. et al. CRMP5 interacts with tubulin to inhibit neurite outgrowth, thereby modulating the function of CRMP2. *J. Neurosci.* **30**, 10639–10654 (2010).
14. Honnorat, J. et al. POP66, a paraneoplastic encephalomyelitis-related antigen, is a marker of adult oligodendrocytes. *J. Neuropathol. Exp. Neurol.* **57**, 311–322 (1998).
15. Honnorat, J., Antoine, J. C., Derrington, E., Aguera, M. & Belin, M. F. Antibodies to a subpopulation of glial cells and a 66 kDa developmental protein in patients with paraneoplastic neurological syndromes. *J. Neurol. Neurosurg. Psychiatry* **61**, 270–278 (1996).
16. Quach, T. T. et al. Molecular cloning of a new unc-33-like cDNA from rat brain and its relation to paraneoplastic neurological syndromes. *Brain Res. Mol. Brain Res.* **46**, 329–332 (1997).
17. Yu, Z. et al. CRMP-5 neuronal autoantibody: marker of lung cancer and thymoma-related autoimmunity. *Ann. Neurol.* **49**, 146–154 (2001).
18. Toikumo, S. et al. A multi-ancestry genetic study of pain intensity in 598,339 veterans. *Nat. Med.* **30**, 1075–1084 (2024).
19. Todd, A. J. Neuronal circuitry for pain processing in the dorsal horn. *Nat. Rev. Neurosci.* **11**, 823–836 (2010).
20. Meyronet, D. et al. Extensive expression of collapsin response mediator protein 5 (CRMP5) is a specific marker of high-grade lung neuroendocrine carcinoma. *Am. J. Surg. Pathol.* **32**, 1699–1708 (2008).
21. Hegazy, M. et al. Proximity ligation assay for detecting protein-protein interactions and protein modifications in cells and tissues in situ. *Curr. Protoc. Cell Biol.* **89**, e115 (2020).
22. Moutal, A. et al. (S)-lacosamide inhibition of CRMP2 phosphorylation reduces postoperative and neuropathic pain behaviors through distinct classes of sensory neurons identified by constellation pharmacology. *Pain* **157**, 1448–1463 (2016).
23. Teichert, R. W., Memon, T., Aman, J. W. & Olivera, B. M. Using constellation pharmacology to define comprehensively a somatosensory neuronal subclass. *Proc. Natl. Acad. Sci. USA* **111**, 2319–2324 (2014).
24. North, R. Y. et al. Electrophysiological alterations driving pain-associated spontaneous activity in human sensory neuron somata parallel alterations described in spontaneously active rodent nociceptors. *J. Pain* **23**, 1343–1357 (2022).
25. Bedi, S. S. et al. Chronic spontaneous activity generated in the somata of primary nociceptors is associated with pain-related behavior after spinal cord injury. *J. Neurosci.* **30**, 14870–14882 (2010).
26. Moutal, A. et al. CRISPR/Cas9 editing of Nf1 gene identifies CRMP2 as a therapeutic target in neurofibromatosis type 1-related pain that is reversed by (S)-Lacosamide. *Pain* **158**, 2301–2319 (2017).
27. Jensen, T. S. & Finnerup, N. B. Allodynia and hyperalgesia in neuropathic pain: clinical manifestations and mechanisms. *Lancet Neurol.* **13**, 924–935 (2014).

28. Truini, A., Garcia-Larrea, L. & Cruccu, G. Reappraising neuropathic pain in humans-how symptoms help disclose mechanisms. *Nat. Rev. Neurol.* **9**, 572–582 (2013).
29. Ponnusamy, R. & Lohkamp, B. Insights into the oligomerization of CRMPs: crystal structure of human collapsin response mediator protein 5. *J. Neurochem* **125**, 855–868 (2013).
30. Faure, F. et al. A pilot study to develop paraneoplastic cerebellar degeneration mouse model. *Cerebellum* **23**, 181–196 (2024).
31. Tanaka, K. et al. Trial to establish an animal model of paraneoplastic cerebellar degeneration with anti-Yo antibody. 2. Passive transfer of murine mononuclear cells activated with recombinant Yo protein to paraneoplastic cerebellar degeneration lymphocytes in severe combined immunodeficiency mice. *Clin. Neurol. Neurosurg.* **97**, 101–105 (1995).
32. Wolff, J. A. et al. Direct gene transfer into mouse muscle in vivo. *Science* **247**, 1465–1468 (1990).
33. Smith, T. R. F. et al. Immunogenicity of a DNA vaccine candidate for COVID-19. *Nat. Commun.* **11**, 2601 (2020).
34. Harte, S. E., Meyers, J. B., Donahue, R. R., Taylor, B. K. & Morrow, T. J. Mechanical conflict system: a novel operant method for the assessment of nociceptive behavior. *PLoS ONE* **11**, e0150164 (2016).
35. Khanna, R. et al. Development and characterization of an injury-free model of functional pain in rats by exposure to red light. *J. Pain* **20**, 1293–1306 (2019).
36. Kagan, L., Turner, M. R., Balu-Iyer, S. V. & Mager, D. E. Subcutaneous absorption of monoclonal antibodies: role of dose, site of injection, and injection volume on rituximab pharmacokinetics in rats. *Pharm. Res.* **29**, 490–499 (2012).
37. Mostkowska, A., Rousseau, G. & Raynal, N. J. Repurposing of rituximab biosimilars to treat B cell mediated autoimmune diseases. *FASEB J.* **38**, e23536 (2024).
38. Dalakas, M. C. B cells as therapeutic targets in autoimmune neurological disorders. *Nat. Clin. Pract. Neurol.* **4**, 557–567 (2008).
39. Moutal, A. et al. CRMP5 controls glioblastoma cell proliferation and survival through notch-dependent signaling. *Cancer Res.* **75**, 3519–3528 (2015).
40. Antoine, J. C. Peripheral neuropathies associated with antibodies directed to intracellular neural antigens. *Rev. Neurol.* **170**, 570–576 (2014).
41. Deng, S. X., Hanson, E. & Sanz, I. In vivo cell penetration and intracellular transport of anti-Sm and anti-La autoantibodies. *Int. Immunol.* **12**, 415–423 (2000).
42. Dalmau, J., Furneaux, H. M., Rosenblum, M. K., Graus, F. & Posner, J. B. Detection of the anti-Hu antibody in specific regions of the nervous system and tumor from patients with paraneoplastic encephalomyelitis/sensory neuronopathy. *Neurology* **41**, 1757–1764 (1991).
43. Fabian, R. H. & Petroff, G. Intraneuronal IgG in the central nervous system: uptake by retrograde axonal transport. *Neurology* **37**, 1780–1784 (1987).
44. Drlicek, M. et al. Circulating antineuronal antibodies reach neurons in vivo: an autopsy study. *J. Neurol.* **239**, 407–410 (1992).
45. Gunasekaran, M. et al. Immunization elicits antigen-specific antibody sequestration in dorsal root ganglia sensory neurons. *Front. Immunol.* **9**, 638 (2018).
46. Gomez, K. et al. Identification and targeting of a unique Na(V)1.7 domain driving chronic pain. *Proc. Natl. Acad. Sci. USA* **120**, e2217800120 (2023).
47. Moutal, A. et al. Dysregulation of CRMP2 post-translational modifications drive its pathological functions. *Mol. Neurobiol.* **56**, 6736–6755 (2019).
48. Dustrude, E. T. et al. Hierarchical CRMP2 posttranslational modifications control NaV1.7 function. *Proc. Natl. Acad. Sci. USA* **113**, E8443–E8452 (2016).
49. Moutal, A. et al. Blocking CRMP2 SUMOylation reverses neuropathic pain. *Mol. Psychiatry* **23**, 2119–2121 (2018).
50. Moutal, A., Luo, S., Largent-Milnes, T. M., Vanderah, T. W. & Khanna, R. Cdk5-mediated CRMP2 phosphorylation is necessary and sufficient for peripheral neuropathic pain. *Neurobiol. Pain* **5**, 100022 (2019).
51. McLaughlin, P. et al. Rituximab chimeric anti-CD20 monoclonal antibody therapy for relapsed indolent lymphoma: half of patients respond to a four-dose treatment program. *J. Clin. Oncol.* **16**, 2825–2833 (1998).
52. Maloney, D. G. et al. Phase I clinical trial using escalating single-dose infusion of chimeric anti-CD20 monoclonal antibody (IDEC-C2B8) in patients with recurrent B-cell lymphoma. *Blood* **84**, 2457–2466 (1994).
53. Keystone, E. et al. Safety and efficacy of additional courses of rituximab in patients with active rheumatoid arthritis: an open-label extension analysis. *Arthritis Rheumatol.* **56**, 3896–3908 (2007).
54. Bomholt, S. F., Mikkelsen, J. D. & Blackburn-Munro, G. Antinociceptive effects of the antidepressants amitriptyline, duloxetine, mirtazapine and citalopram in animal models of acute, persistent and neuropathic pain. *Neuropharmacology* **48**, 252–263 (2005).
55. Fernihough, J. et al. Pain related behaviour in two models of osteoarthritis in the rat knee. *Pain* **112**, 83–93 (2004).
56. Iyengar, S., Webster, A. A., Hemrick-Luecke, S. K., Xu, J. Y. & Simmons, R. M. Efficacy of duloxetine, a potent and balanced serotonin-norepinephrine reuptake inhibitor in persistent pain models in rats. *J. Pharmacol. Exp. Ther.* **311**, 576–584 (2004).
57. Hunter, J. C. et al. The effect of novel anti-epileptic drugs in rat experimental models of acute and chronic pain. *Eur. J. Pharmacol.* **324**, 153–160 (1997).
58. Millecamps, M., Etienne, M., Jourdan, D., Eschalier, A. & Ardid, D. Decrease in non-selective, non-sustained attention induced by a chronic visceral inflammatory state as a new pain evaluation in rats. *Pain* **109**, 214–224 (2004).
59. François-Moutal, L. et al. A membrane-delimited N-myristoylated CRMP2 peptide aptamer inhibits CaV2.2 trafficking and reverses inflammatory and postoperative pain behaviors. *Pain* **156**, 1247–1264 (2015).
60. Yaksh, T. L. & Rudy, T. A. Chronic catheterization of the spinal subarachnoid space. *Physiol. Behav.* **17**, 1031–1036 (1976).
61. Chaplan, S. R., Bach, F. W., Pogrel, J. W., Chung, J. M. & Yaksh, T. L. Quantitative assessment of tactile allodynia in the rat paw. *J. Neurosci. Methods* **53**, 55–63 (1994).
62. Hargreaves, K., Dubner, R., Brown, F., Flores, C. & Joris, J. A new and sensitive method for measuring thermal nociception in cutaneous hyperalgesia. *Pain* **32**, 77–88 (1988).
63. Ulmer, J. B. et al. Heterologous protection against influenza by injection of DNA encoding a viral protein. *Science* **259**, 1745–1749 (1993).
64. Colluru, V. T. & McNeel, D. G. B lymphocytes as direct antigen-presenting cells for anti-tumor DNA vaccines. *Oncotarget* **7**, 67901–67918 (2016).
65. Geiben-Lynn, R. et al. CD4+ T lymphocytes mediate in vivo clearance of plasmid DNA vaccine antigen expression and potentiate CD8+ T-cell immune responses. *Blood* **112**, 4585–4590 (2008).
66. Khawaja, G. et al. Enhanced magnitude and breadth of neutralizing humoral response to a DNA vaccine targeting the DHBV envelope protein delivered by in vivo electroporation. *Virology* **425**, 61–69 (2012).
67. Sparwasser, T. et al. Bacterial DNA and immunostimulatory CpG oligonucleotides trigger maturation and activation of murine dendritic cells. *Eur. J. Immunol.* **28**, 2045–2054 (1998).
68. Davis, H. L. Intramuscular and intradermal injection of DNA vaccines in mice and primates. *Methods Mol. Med.* **29**, 71–77 (2000).

Acknowledgements
L.M. and H.J.S. are co-first authors. Their contribution to this research was equal and is named in alphabetical order. We thank Mid-America Transplant and Dr. Grant Kolar for their support in facilitating access to human DRG. This research was supported by startup funds from Saint Louis University, National Institutes of Health NINDS R01NS119263, R01NS119263-04S1 to A.M., and NINDS R01NS098772 and R01NS120663, NIDA DA042852 to R.K. We are grateful to Genentech for sharing their anti-CD20 monoclonal antibody. Most authors completed this work while at the University of Arizona. L.D.D., V.R., and J.H. are supported by a public grant overseen by the *Agence Nationale de la Recherche* (ANR; French research agency) as part of the *Investissements d'Avenir* program (ANR-18-RHUS-0012), also performed within the framework of the LABEX CORTEX of the Université Claude Bernard Lyon 1 (program *Investissements d'Avenir*, ANR-11-LABX-0042, operated by the ANR), and also supported by the European Reference Network RITA. Current affiliations are as follows, H.J.S.: Pittsburgh Center for Pain Research, University of Pittsburgh, Pittsburgh, PA 15213, USA; K.G., S.L.L., A.C.R., and R.K.: Department of Department of Pharmacology & Therapeutics, College of Medicine, University of Florida, Gainesville, FL 32610 USA; C.T.: The National and Local Joint Engineering Laboratory of Animal Peptide Drug Development, College of Life Sciences, Hunan Normal University, Changsha, 410081, China; D.R.: Department of Pharmacology, School of Pharmacy, Chongqing Medical University, Chongqing 400016, China; S.S.B.: Medical Scientist Training Program (MSTP), Mayo Clinic, Rochester, MN, USA.

Author contributions
L.M., N.L.A.D., and S.L. performed behavior experiments on rats; H.J.S., L.Y.S., K.G., S.L.L., C.T., A.C.R., and D.R. performed electrophysiological recordings; L.D.D., N.L.A.D., and V.N. performed fluorescence imaging; V.N. performed ELISA, S.S.B. and A.M. performed calcium imaging; L.F.M. and A.M. performed epitope mapping with peptide arrays; V.R. and J.H. provided the serum samples with CV2/CRMP5-Abs and patient information; L.M., H.J.S., N.L.A.D., L.Y.S., K.G., L.D.D., S.S.B., L.F.M., F.P, M.I., J.H., R.K., and A.M. analyzed data; R.K. and A.M. conceptualized the research, L.M., H.J.S., L.F.M., K.G., R.K., and A.M., designed experiments, A.M., R.K., F.P., M.I., J.H., L.F.M., L.M., and H.J.S wrote and revised the manuscript.

Competing interests
The authors declare no competing interests.

Additional information
Supplementary information The online version contains supplementary material available at https://doi.org/10.1038/s41467-025-62380-y.

Correspondence and requests for materials should be addressed to Aubin Moutal.

Peer review information *Nature Communications* thanks the anonymous reviewer(s) for their contribution to the peer review of this work. A peer review file is available.